17

Higgs particles

17.1 Higgs-boson couplings

The electroweak theory depends crucially on the Higgs mechanism. Many aspects of the theory have been tested in experiments to a high degree of accuracy, especially properties of the gauge bosons and their couplings to fermions. However, the Higgs particles have not been discovered yet. In Chapter 7 we discussed the simplest and, perhaps, the most natural way of breaking the SU(2) symmetry, namely by introducing a doublet of scalar particles. Among them three fields were eliminated, becoming the longitudinal degrees of freedom for the gauge bosons. The remaining neutral particle is physical and should be observed. In the same chapter it was shown that giving the Higgs field a vacuum expectation value generates masses for $W^{\pm}$ and Z^0, whose ratio is related to the weak mixing angle. This ratio has been confirmed experimentally, which provides strong support for the underlying SU(2) symmetry.

The Higgs doublet contains two complex fields:

$$\begin{pmatrix} \phi^+ \\ \phi^0 \end{pmatrix}. \tag{17.1}$$

The breaking of the symmetry introduces the vacuum expectation value

$$\langle \phi^0 \rangle = \frac{v}{\sqrt{2}}. \tag{17.2}$$

The scalar Lagrangian introduced in Chapter 7 has two parameters, μ and λ, which are related to the value of the field at the minimum:

$$v = \frac{\mu}{\sqrt{\lambda}} = \left(\sqrt{2}G\right)^{-\frac{1}{2}}.$$

https://doi.org/10.1017/9781009402378.018 Published online by Cambridge University Press

The expansion of the field around the minimum of the potential

$$\phi' = \frac{1}{\sqrt{2}} \begin{pmatrix} 0 \\ v + H \end{pmatrix} \tag{17.3}$$

introduces the physical field H as a fluctuation around the minimum. The numerical value of v was determined in Eq. (8.20), leaving the mass of the scalar as the only undetermined parameter of the Higgs sector,

$$\frac{M_{\mathrm{H}}^2}{2} = -\frac{\mu^2}{2} + \frac{3}{2}\lambda v^2 = \mu^2. \tag{17.4}$$

Consequently, all couplings of the Higgs particles are rewritten in terms of M_{H} and other coupling constants already determined in previous chapters. After a short study of the couplings, one finds

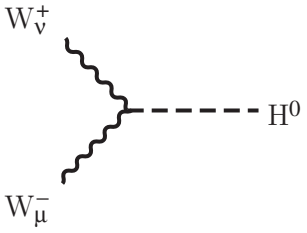

$$\mathrm{i}g M_{\mathrm{W}} g_{\mu\nu}$$

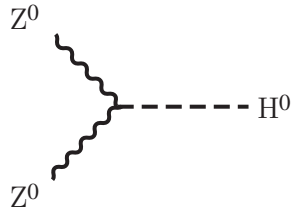

$$\frac{\mathrm{i}g M_{\mathrm{Z}}}{\cos\theta_{\mathrm{W}}} g_{\mu\nu}$$

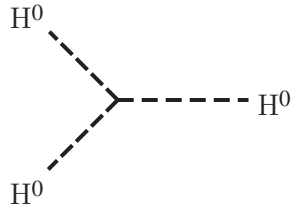

$$-\mathrm{i}3!\lambda v$$

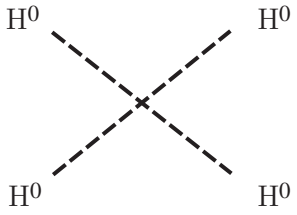

$$-\mathrm{i}3!\lambda$$

https://doi.org/10.1017/9781009402378.018 Published online by Cambridge University Press

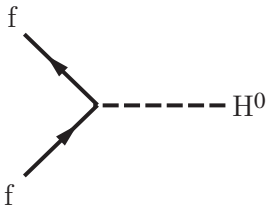

$$\frac{-\mathrm{i}m_{\mathrm{f}}}{v}$$

with

$$v = \frac{\mu}{\sqrt{\lambda}} = (\sqrt{2}G)^{-1/2} = 246\,\mathrm{GeV}.$$

With so many couplings depending on a single parameter, we can proceed to calculate the decays of Higgses to other particles as well as their production cross sections. In this way we find processes in which the Higgs particles must be produced, provided that they are not very heavy, or they should appear in the decay of ordinary or new heavy particles. All these approaches have been pursued actively, but no Higgs particles have been discovered yet. Instead we have bounds on their masses and the production rates. We shall cover several of these topics in this chapter.

A very important role in all such studies is played by the Higgs mass. There are efforts to limit the mass by appealing to unitarity or demanding that the electroweak theory remains renormalizable. An alternative direction of investigation studies the effects introduced by radiative corrections to several processes. Higgs particles, together with quarks and gauge bosons, appear as intermediate states of Feynman diagrams. Many experiments have reached a high level of accuracy so that radiative corrections must be included in order to bring agreement between theory and experiment. They provide a crucial test of the theory and impose constraints on the Higgs mass. We study several of them in the next section.

17.2 Precision tests of the theory

The electroweak theory introduces several parameters that are undetermined. Among them are the mass of the Higgs and the masses and mixing angles of the fermions. The gauge couplings and the masses of the gauge bosons enter in many reactions, where they are determined precisely to have the same value. As two examples we mention the weak mixing angle $\sin^2\theta_{\mathrm{W}}$ and the Fermi coupling constant. They have been measured in various reactions so precisely that higher-order corrections are necessary. The loop corrections include quantum corrections of the theory testing it to a higher degree of accuracy. In this section we review the precise measurements for several parameters and point out reactions where

https://doi.org/10.1017/9781009402378.018 Published online by Cambridge University Press

discrepancies may appear on the horizon. At present the agreement is so good that we can consider the results from such tests a great success of the theory.

In order to make predictions, we use three quantities as input parameters. They are defined in various processes where they can be determined precisely, including radiative corrections, and then they are used to predict other processes.

(i) The first is the fine-structure constant α measured in experiments that involve the Josephson junction or the anomalous magnetic moment of the electron. It receives corrections from strong interactions and varies with the momentum at which it is measured in a way similar to the strong coupling constant described in Section 11.2.
(ii) The second parameter is the Fermi coupling constant determined from the muon lifetime. The corrections include electromagnetic and weak effects.
(iii) As a third parameter, we can select one of the masses M_{W} or M_{Z}. It is customary to choose M_{Z} determined from the Z lineshape, because it has been measured more accurately.

With these three parameters we can predict other quantities. For instance,

$$\sin^2\theta_{\mathrm{W}}\,\cos^2\theta_{\mathrm{W}} = \frac{\pi\alpha}{\sqrt{2}G_{\mathrm{F}}}\frac{1}{M_{\mathrm{Z}}^2} \tag{17.5}$$

and $M_{\mathrm{W}} = M_{\mathrm{Z}}\cos\theta_{\mathrm{W}}$, which is also rewritten as

$$\rho = \frac{M_{\mathrm{W}}^2}{M_{\mathrm{Z}}^2\cos^2\theta_{\mathrm{W}}} = 1. \tag{17.6}$$

The ρ parameter determines the strength of neutral currents relative to charge currents and to lowest order (tree level) it has the value unity. It is modified by corrections, as we will mention below. Measuring quantities and carrying out precision tests of the theory is a research field in itself. I decided to present here the general features that enter such calculations and mention a few comparisons, especially those for which there are small disagreements. The reader who wishes to specialize in this field can consult the corresponding section in the particle data group (Erler and Langacker, 2004) or books devoted to this topic (Bardin and Passarino, 1999).

We have seen in previous chapters that one-loop radiative corrections involve integrals of the form

$$\int \mathrm{d}^4k\,\frac{1}{(k^2+m^2+\mathrm{i}\varepsilon)^\alpha} \tag{17.7}$$

(see, for instance, Sections 14.7 and (15.7)). When $\alpha \leq 2$ the integral diverges. In a renormalizable theory the infinities are absorbed as corrections to masses and coupling constants. Since they are arbitrary, it appears, at first glance, that the corrections are unobservable. An exception to this rule occurs when masses and

https://doi.org/10.1017/9781009402378.018 Published online by Cambridge University Press

Figure 17.1. Self-energies for gauge bosons.

coupling are not free but are related to each other. As a first example, we mention the equality of the vector couplings occurring in muon decay and β-decay. They are used to determine a precise value for V_{ud} as given in Section 9.3.1.

Another accurate example is provided by the ρ parameter in Eq. (17.6). It receives corrections from the self-energies shown in Fig. 17.1, where the intermediate solid lines represent quarks and the dotted lines Higgs bosons. It is sensitive to the masses of particles in the intermediate states and provided a benchmark for restricting the masses of these particles. The above-mentioned corrections give rise to deviations from unity given by the equation

$$\rho = 1 + \frac{G_F}{8\pi^2}\left[m_1^2 + m_2^2 - \frac{2m_1^2 m_2^2}{m_2^2 - m_1^2}\ln\left(\frac{m_2^2}{m_1^2}\right) - \frac{3M_W \sin^2\theta_W}{\cos^2\theta_W}\ln\left(\frac{M_H^2}{M_W^2}\right)\right], \quad (17.8)$$

with m_2 and m_1 the masses of the top and bottom quarks, respectively, and M_H the mass of the Higgs boson. Other quark pairs also contribute, but the magnitude of their correction is smaller.

With the above inputs, $\sin^2\theta_W$ and M_W can be calculated when values for m_t^2 and M_H are given. Such arguments were used to constrain the top quark's mass before its discovery. Experimental results from the Large Electron–Positron Collider (LEP) combined with loop contributions restricted the mass m_t to within the range 160–180 GeV where the top quark was discovered. The standard-model prediction now is

$$m_t(m_t) = 174.3 \pm 3.4\,\text{GeV}. \quad (17.9)$$

Furthermore, the precision electroweak data accumulated at the LEP, SLAC, and the Tevatron strongly support the standard model with a weakly coupled Higgs boson. As described above, the Higgs boson contributes to the $W^{\pm}$ and Z vacuum polarization through loop effects. The result of a global fit is shown in Fig. 17.2 and yields the value (Eidelman, 2004)

$$M_H = 126^{+73}_{-48}\,\text{GeV}, \quad (17.10)$$

which is consistent with the lower bound of 114.4 GeV established in direct searches. These values provide a benchmark for designing experiments aiming at the discovery of the Higgs particles.

https://doi.org/10.1017/9781009402378.018 Published online by Cambridge University Press

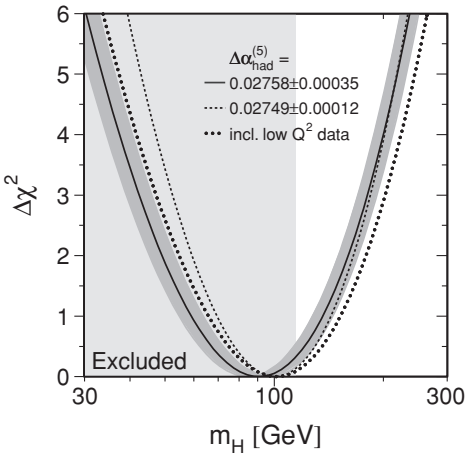

Figure 17.2. The result of the global fit presented as $\Delta\chi^2 = \chi^2 - \chi^2_{\min}$ versus M_H.

Before leaving this section, it is worth mentioning two cases in which, if we look at the results in detail, they are either not satisfactory or could indicate small disagreements with the predictions of the standard model. A neutrino experiment at Fermilab completed a precise measurement of $\sin^2\theta_W$ using the R ratio of Eq. (12.17) and other ratios. A 3σ deviation from the standard-model prediction was reported. This conclusion depends on several theoretical parameters entering the analysis that are now under active investigation (Gluck *et al.*, 2005).

A further discrepancy appears in the determination of the effective weak mixing angle. The adjective "effective" indicates that a specific renormalization scheme has been introduced for the higher-order corrections. The two most precise measurements of $\sin^2\theta_{eff}$ from SLAC from polarized-electron asymmetry A_{LR} and from the forward–backward asymmetry A^b_{FB} in the production of b–$\bar{b}$ pairs differ by $\sim 3\sigma$. In fact, the result from A_{LR} is in good agreement with the leptonic asymmetries measured at the LEP, whereas all other hadronic asymmetries are better compatible with the A^b_{FB}.

Besides the efforts for discovering the Higgs bosons, it is also important to confirm or eliminate these discrepancies. There are theoretical corrections that have been pointed out and are being actively discussed. Their implications are so profound that one should continue the investigations. The absence of Higgs particles in the mass range discussed in this section and/or the persistence of the discrepancies will be an indication of new physics. A promising candidate for new physics is supersymmetry, whose presence is capable of modifying the predictions described in this section.

https://doi.org/10.1017/9781009402378.018 Published online by Cambridge University Press

17.3 Bounds on masses from general principles

There are many new reactions that are possible in the electroweak theory. At tree level the amplitudes involve a few partial waves and must satisfy unitarity bounds. For elastic WW scattering the bounds have been exploited effectively to restrict the mass of the Higgs boson.

At very high energies the longitudinal polarization of the W bosons is $\varepsilon_{\mathrm{L}}^{\mu} \approx p^{\mu}/M_{\mathrm{W}}$. It produces the fastest growing amplitudes as functions of energy and involves one partial wave. The scattering amplitude can be expanded in terms of partial waves:

$$M(s,t) = \frac{1}{k}\sum_{\ell=0}^{\infty}(2\ell+1)a_{\ell}(s)P_{\ell}(\cos\theta). \tag{17.11}$$

The fact that each partial wave must satisfy a unitarity bound leads to the condition

$$|a_0| \leq \frac{1}{2} \tag{17.12}$$

and supplies an upper bound for the mass of the Higgs boson (Lee *et al.*, 1977),

$$M_{\mathrm{H}}^2 < \frac{4\pi\sqrt{2}}{G_{\mathrm{F}}} \approx (1.2\,\mathrm{TeV})^2. \tag{17.13}$$

This is the simplest bound described also in Problem 2. It can be improved (Lee *et al.*, 1977) by considering the coupled channels $\mathrm{W_L W_L}$, $\mathrm{Z_L Z_L}$, $\mathrm{Z_L H}$, and HH, with the subscript L indicating longitudinal polarization, then demanding that the eigenvalues of these coupled channels satisfy the unitarity conditions. The improved bound is smaller by a factor of $1/\sqrt{3}$, i.e.

$$M_{\mathrm{H}} \leq 700\,\mathrm{GeV}.$$

New bounds are obtained by requiring stability of the vacuum. We saw in Chapter 5 that the Higgs potential must have the specific form of Fig. 5.1 in order to be able to expand the field around a minimum of the potential. This property must be preserved even when radiative corrections are included. The coupling constant λ receives corrections from loop diagrams and it becomes a "running" coupling depending on the scale Λ at which it is evaluated. The change of λ is given by a differential equation that depends on the Yukawa coupling (quark loops) and the gauge coupling (gauge loops). The corrected potential has the form

$$V_{\mathrm{eff}} = -\mu^2 H^2 + \lambda(\Lambda)H^4 \tag{17.14}$$

and its minimum defines again a vacuum expectation value: $\langle\phi\rangle = v/\sqrt{2}$. If the corrections are large, it is possible to obtain a negative λ and consequently

https://doi.org/10.1017/9781009402378.018 Published online by Cambridge University Press

an unstable ground state. On the other hand, for λ large and positive there is one trivial minimum at the origin. Since $V(0) = 0$, a non-trivial minimum exists provided that $V(v/\sqrt{2}) < 0$. This condition gives the lower bound (Linde, 1976)

$$M_{\mathrm{H}} \gtrsim 50\,\mathrm{GeV} \quad \text{with} \quad \Lambda = 1\,\mathrm{TeV}.$$

Experimental searches for Higgses have gone much above this value. The best value available comes from the reaction in Eq. (17.15) to be discussed later on.

17.4 Decays

At the beginning of this chapter we listed several couplings that depend on a single parameter M_{H}. A characteristic property in models with one Higgs doublet is that Higgs particles couple strongly to the heaviest particle. For instance, the couplings to fermions prefer the top quark and the couplings to W and Z bosons are proportional to their masses. With so many couplings available, it is straightforward to compute decay widths and production rates. We list in Table 17.1 decay widths for several channels.

The decays have special properties worth mentioning. The lifetime of the Higgs particle is very short and, being neutral, it leaves no visible track. Its decay products, such as $\mathrm{b\bar{b}}$ or $\tau\tau$ pairs, produce detectable tracks. They are used as signatures for discovering the Higgs boson.

The decays to vector mesons also have several interesting properties. The formulas for decay widths into the weak vector bosons Z and W look quite similar, except for an additional factor of $\frac{1}{2}$, accounting for the symmetric final state in the case of two identical Z bosons. In the limit $m_{\mathrm{Z}}, m_{\mathrm{W}} \ll m_{\mathrm{H}}$ the width of the ZZ pairs is half of the $\mathrm{W^+W^-}$ width. The vector bosons have three polarizations and it is interesting to investigate the decays to final states with specific polarizations. The longitudinal polarizations are created by the Higgs particles and may show irregularities. For large Higgs masses the vector bosons in the final state are dominantly longitudinally polarized, which may be important for distinguishing this process from the background.

The decays into fermions or weak vector bosons proceed through tree diagrams, in contrast to the decays in groups (4) and (5), which contain loop contributions. For loop contributions one expects the branching ratios to be smaller, which is indeed the case. However, for $M_{\mathrm{H}} \leq 200\,\mathrm{GeV}$ they are still measurable because the sum over all possible particles inside the loop brings an enhancement. The gluonic decays are drowned in a huge background, in contrast to photonic decays with two stable particles, which provide a convenient way for identifying the Higgs. Both

https://doi.org/10.1017/9781009402378.018 Published online by Cambridge University Press

Table 17.1. *Partial decay widths of the Higgs boson*

Higgs boson H decays into ...	Partial decay width Γ with $\lambda_i = m_i^2/m_{\mathrm{H}}^2$
(1) fermions f: $\mathrm{H} \to \mathrm{f}\bar{\mathrm{f}}$	$N_{\mathrm{c}} \dfrac{G_{\mathrm{F}}}{4\pi\sqrt{2}} m_{\mathrm{f}}^2 m_{\mathrm{H}} (1 - 4\lambda_{\mathrm{f}})^{3/2}$ N_{c} is a color factor; $N_{\mathrm{c}} = \begin{cases} 1 \text{ for leptons} \\ 3 \text{ for quarks} \end{cases}$
(2) weak neutral bosons Z^0: $\mathrm{H} \to \mathrm{Z}^0\mathrm{Z}^0$	$\dfrac{G_{\mathrm{F}}}{16\pi\sqrt{2}} m_{\mathrm{H}}^3 (1 - 4\lambda_{\mathrm{Z}})^{1/2} \left(12\lambda_{\mathrm{Z}}^2 - 4\lambda_{\mathrm{Z}} + 1\right)$
(3) weak charged bosons $\mathrm{W}^{\pm}$: $\mathrm{H} \to \mathrm{W}^+\mathrm{W}^-$	$\dfrac{G_{\mathrm{F}}}{8\pi\sqrt{2}} m_{\mathrm{H}}^3 (1 - 4\lambda_{\mathrm{W}})^{1/2} \left(12\lambda_{\mathrm{W}}^2 - 4\lambda_{\mathrm{W}} + 1\right)$
(4) gluons g: $\mathrm{H} \to \mathrm{gg}$ (via a loop containing quarks q)	$\dfrac{G_{\mathrm{F}}}{36\pi\sqrt{2}} m_{\mathrm{H}}^3 \left[\dfrac{\alpha_{\mathrm{s}}(m_{\mathrm{H}^0}^2)}{\pi}\right]^2 \left\lvert \sum_q I_q \right\rvert^2$ with $I_q = 3\left[2\lambda_q + \lambda_q(4\lambda_q - 1) f(\lambda_q)\right]$ $f(\lambda) = \begin{cases} -2\left[\sin^{-1}(1/\sqrt{4\lambda})\right]^2, & \lambda > 1/4 \\ \frac{1}{2}\left[\ln(\eta^+/\eta^-) - \mathrm{i}\pi\right]^2, & \lambda < 1/4 \end{cases}$ $\eta^{\pm} = 1/2 \pm \sqrt{1/4 - \lambda}$
(5) photons γ: $\mathrm{H} \to \gamma\gamma$	$\dfrac{G_{\mathrm{F}}}{8\pi\sqrt{2}} m_{\mathrm{H}}^3 \left(\dfrac{\alpha}{\pi}\right)^2 \lvert I \rvert^2$ with $I = \sum_q Q_q^2 I_q + \sum_l Q_l^2 I_l + I_{\mathrm{W}} (+ I_{\mathrm{s}})$ Q_i is the charge of particle i and $I_q = 3\left[2\lambda_q + \lambda_q(4\lambda_q - 1) f(\lambda_q)\right]$ $I_l = 2\lambda_l + \lambda_l(4\lambda_l - 1) f(\lambda_l)$ $I_{\mathrm{W}} = 3\lambda_{\mathrm{W}}(1 - 2\lambda_{\mathrm{W}}) f(\lambda_{\mathrm{W}}) - 3\lambda_{\mathrm{W}} - 1/2$ $I_{\mathrm{s}} = -\lambda_{\mathrm{s}}[1 + 2\lambda_{\mathrm{s}} f(\lambda_{\mathrm{s}})]$

photonic and gluonic modes proceed through loop diagrams; some of them are shown in Fig. 17.3 (Gunion *et al.*, 1990; Hinchlife, 1998).

The relative importance of various decays depends on the mass of the Higgs particles. We present in Table 17.2 dominant decays to various modes as a function of the Higgs mass. In the low-mass range the decay to $\mathrm{b\bar{b}}$ pairs dominates and is identified by its decay products. The decay to $\gamma\gamma$ is less frequent ($\sim 10^{-3}$) but has a smaller background. For higher masses, decays to gauge bosons dominate.

https://doi.org/10.1017/9781009402378.018 Published online by Cambridge University Press

Table 17.2. *Higgs decay modes as a function of its mass*

m_H (GeV)	Decay
90–120	$H \to b\bar{b}, \gamma\gamma$
120–140	$H \to b\bar{b}, WW^*, \tau^+\tau^-$
140–180	$H \to b\bar{b}, WW^*, ZZ^*, \tau^+\tau^-$
180–380	$H \to WW, ZZ$
>380	$H \to WW, ZZ, t\bar{t}$

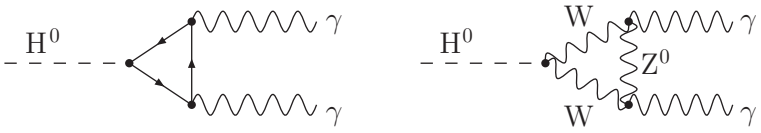

Figure 17.3. Some triangle diagrams for decay of a Higgs boson to photons.

Some decay modes may contribute even below the threshold for pair production of gauge bosons because some of them are present as virtual intermediate states. We denote them with a star as superscript; for instance W^*, which subsequently decays to $e^-\bar{\nu}$.

The calculation of decays proceeding through tree diagrams involves a matrix element and a two-body phase space, which are straightforward to calculate. We suggest some of them as exercises at the end of the chapter.

17.5 Production in electron–positron colliders

The discovery of the Higgs particle is of paramount importance. For this reason there have been large experiments designed to discover them. The early expectations of a light Higgs have been ruled out experimentally. A light Higgs appears in the decay of the known particles, like mesons, charmonium, and the gauge bosons. Intensive searches in these decays did not produce any evidence for Higgs particles. The next possibility is to produce them in electron–positron colliders through the process shown in Fig. 17.4:

$$e^+e^- \to V^* \to V + H \qquad \text{with} \quad (V = W, Z) \\ \qquad\qquad\qquad\quad \hookrightarrow \text{leptons} \tag{17.15}$$

https://doi.org/10.1017/9781009402378.018 Published online by Cambridge University Press

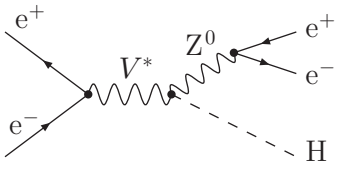

Figure 17.4. Bremsstrahlung from weak bosons.

which is known as bremsstrahlung from the weak gauge bosons. For lower energies ($\sqrt{s} \approx 200$–500 GeV) bremsstrahlung dominates and has been searched for at the LEP collider at CERN. The cross section is maximal at center-of-mass energies close to the Z resonance, where it is given by (Gunion *et al.*, 1990)

$$\sigma(\mathrm{e^+e^-} \to \mathrm{ZH}) = \frac{G_\mathrm{F}^2 M_\mathrm{Z}^4}{96\pi}\left[1 + (1 - 4\sin^2\theta_\mathrm{W})^2\right]\frac{8k}{\sqrt{s}}\left[\frac{k^2 + 3M_\mathrm{Z}^2}{\left(s - M_\mathrm{Z}^2\right)^2 + M_\mathrm{Z}^2\Gamma^2}\right]. \tag{17.16}$$

Here k is the center-of-mass momentum of the Z boson produced. The detection of this channel observes the outgoing Z and reconstructs the Higgs boson's invariant mass as

$$M_\mathrm{H}^2 = s - 2\sqrt{s}E_\mathrm{Z} + M_\mathrm{Z}^2. \tag{17.17}$$

The searches at CERN established the bound

$$M_\mathrm{H} > 114.4\,\mathrm{GeV}.$$

A similar process occurs in hadron colliders, where the initial leptons are replaced by quarks to give

$$\mathrm{q\bar{q}} \to V^* \to V + \mathrm{H}.$$

For center-of-mass energies higher than 500 GeV, the fusion process

$$\mathrm{e^+e^-} \to \nu\bar{\nu} + \mathrm{H},$$

shown in Fig. 17.5, begins to dominate. For high energies the initial partons or leptons radiate not only photons but also W and Z gauge bosons. Here one must be careful to include all possible diagrams in order to satisfy gauge invariance. The calculation follows a method very similar to that for the emission of photons, in the Weizsacker–Williams approximation, with special attention paid to the longitudinal and transverse polarization (Gunion *et al.*, 1990). In this way one derives an effective

https://doi.org/10.1017/9781009402378.018 Published online by Cambridge University Press

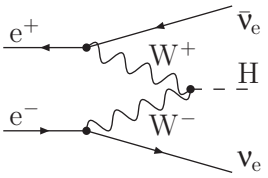

Figure 17.5. W–W fusion.

W-emission approximation, which leads to the cross section (Wilczek, 1977; Cahn and Dawson, 1984; Jones and Petkov, 1979)

$$\sigma(e^+e^- \to \nu\bar{\nu}H) \approx \frac{G_F^3 M_W^4}{4\sqrt{2}\pi^3}\left[\ln\left(\frac{s}{M_H^2}\right) - 2\right]. \tag{17.18}$$

This reaction is attractive because it has a low background. It starts smaller than the bremsstrahlung reaction in Eq. (17.15), but grows with increasing energy to become dominant at $\sqrt{s} \approx 500\,\text{GeV}$.

Finally, it is possible to create the Higgs particle in photon fusion:

$$\gamma\gamma \to H \to b\bar{b}.$$

For low-energy photons this process is very small. However, for intense high-energy laser beams it has a resonance structure and may become important. For Higgs masses larger than 150 GeV the dominant final states are two gauge bosons.

17.6 Production in hadron colliders

The high-energy electron–positron collider (LEP) completed its runs and set the bound of 114.4 GeV. The next searches will be taking place in hadron colliders. Searches are already taking place at the Tevatron and a large hadron collider (LHC) is under construction at CERN. Several of the reactions in the previous section become hadronic reactions once we replace the initial leptons by quarks or quark–antiquark pairs.

In hadronic collisions the process of gluon fusion is the most important source for Higgs-particle production. In this process the Higgs couples via a quark triangle diagram to the gluons. The point-like cross section at parton level is (Kniehl, 1994)

$$\sigma(gg \to H) = \frac{\pi^2}{8}\frac{\Gamma(H \to gg)}{M_H}\delta\left(\hat{s} - M_H^2\right). \tag{17.19}$$

For the total hadronic cross section it is very important to take higher-order gluonic corrections into account, because their contribution is positive and increases the

https://doi.org/10.1017/9781009402378.018 Published online by Cambridge University Press

cross section. The cross section decreases with increasing Higgs mass, although the Yukawa coupling grows with the loop-quark mass.

At the Tevatron, a $\bar{\text{p}}\text{p}$ collider at Fermilab, the two efficient mechanisms are gluon fusion and associated production with a W or a Z:

$$\text{gg} \to \text{H} \to \text{b}\bar{\text{b}}, \tag{17.20}$$

$$\text{q}\bar{\text{q}} \to \text{W}^*/\text{Z}^* \to \text{W}/\text{Z} + \text{H}. \tag{17.21}$$

Although the gg process has the larger cross section, ~ 1 pb (one picobarn) at $M_{\text{H}} = 115$ GeV, it is hard to detect it for $M_{\text{H}} < 130$ GeV. In this mass range the dominant decay is $\text{H} \to \text{b}\bar{\text{b}}$ (see Fig. 1 in Hinchlife (1998)), which is swamped by a multijet background. For these masses only the production of a Higgs in association with a vector boson has enough sensitivity. The WH and ZH channels give a clear signal with lepton(s), missing neutrino(s) and two b-jets. The searches continue at the Tevatron, where there are plans to reach an integrated luminosity of $\sim 8\,\text{fb}^{-1}$.

The Tevatron has the potential of discovering the standard-model Higgs with masses less than ~170 GeV. Heavier Higgses must wait for the LHC, which will reach a center-of-mass energy of 14 TeV. It will run for an integrated luminosity of $300\,\text{fb}^{-1}$ and can discover Higgs particles with masses up to $1\,\text{TeV} = 10^3$ GeV. At these high energies, in addition to the gluon–gluon fusion, the quarks radiate gauge bosons. A new process of W–W fusion into Higgs, analogous to the one shown in Fig. 17.5,

$$\text{W} + \text{W} \to \text{H} \to \gamma\gamma,\ \text{ZZ}^*, \ldots \tag{17.22}$$

becomes significant. If the standard-model Higgs has a mass above twice the Z mass, the discovery will be through the channel

$$\text{pp} \to \text{H} + \text{hadrons} \to \text{ZZ} + \cdots \to (l^+l^-)(l^+l^-) + \cdots. \tag{17.23}$$

This is called the golden channel for Higgs production and decays. Both lepton pairs will have the mass of the Z boson, making possible the reduction of many backgrounds.

If the mass of the Higgs boson is much bigger than the mass of the W or Z boson, $M_{\text{H}} \gg 2M_{\text{W}}$, the width is

$$\Gamma(\text{H} \to \text{WW}) \approx \frac{3G_{\text{F}}}{16\pi\sqrt{2}} M_{\text{H}}^3 \approx 0.48\,\text{TeV}\left(\frac{M_{\text{H}}}{1\,\text{TeV}}\right)^3. \tag{17.24}$$

This width grows rapidly with the mass of the Higgs particle and is very broad for

https://doi.org/10.1017/9781009402378.018 Published online by Cambridge University Press

large masses. The increased width of the Higgs and the reduced production rate determine the upper limit for detecting a heavy Higgs.

17.7 Other symmetry-breaking schemes

There is so much supporting evidence for a Higgs particle with a mass lower than 1 TeV that the chances of discovering it at the LHC are very high. If the Higgs is not of the simple form discussed in this chapter, there are strong arguments from unitarity and from higher-order corrections that another mechanism must be operating to reduce the fast growth of amplitudes and cross sections. Thus either the Higgs will show up as the simple scalar of the standard model, or a more complicated structure must appear.

Extensions of the standard model can have more complicated spectra of Higgs bosons. A popular extension is supersymmetry with two Higgs doublets whose neutral components have two vacuum expectation values. The physical particles are now a charged boson ($H^{\pm}$), two neutral scalar Higgses (H_1^0 and H_2^0), and one pseudoscalar (A) (Hinchlife, 1998).

Charged Higgs bosons can be pair-produced in e^+e^- and $q\bar{q}$ annihilation. The chance of detecting them depends on the energy of the collider and the branching ratios to $\nu\tau$, $c\bar{s}$, and $c\bar{b}$. Searches at the LEP did not discover them and thereby set upper limits on their masses.

In the simplest version of the supersymmetric model the mass of the lightest neutral scalar depends on the top quark's mass, the ratio of the two vacuum expectation values, and the masses of other supersymmetric particles. For $M_{\text{top}} = 175\,\text{GeV}$, there is a bound $M_{H_1^0} \lesssim 130$ GeV, provided that the ratio of the vacuum expectation values is large. This mass is within the range of the Tevatron and LHC, as we discussed earlier.

We mention a final possibility, whereby the Higgs particle is a bound state of quark–antiquark pairs. In such theories a new strong interaction must be present to bind the quark pair together. A dynamical symmetry breaking has been formulated with a top-quark condensate (Bardeen *et al*., 1996), in analogy with the BCS theory of superconductivity. The low-energy effective theory is the standard model supplemented with relationships connecting masses of the top quark, W boson, and Higgs boson.

Another extension introduces new quarks (techniquarks) coupled to W and Z bosons and bound together by new gluons, the technigluons. There is a new coupling constant, which runs to become strong at a scale $\sim$1 TeV. The theory is a scaled-up version of QCD with heavy fermions U and D imitating the light up and down quarks. The strong interactions at 1 TeV cause a spontaneous breaking of the $SU(2)_L \times SU(2)_R$ symmetry of the new quarks, producing heavy color scalars – the

https://doi.org/10.1017/9781009402378.018 Published online by Cambridge University Press

new Goldstone bosons (Fahri and Susskind, 1979). Searches for the new scalars follow the methods we described in this and the previous section.

Problems for Chapter 17

1. Show that the decay rates to transverse ($\pm$) and longitudinally (L) polarized W bosons are

$$\Gamma(\mathrm{H}^0 \to \mathrm{W}_+\mathrm{W}_+) = \Gamma(\mathrm{H}^0 \to \mathrm{W}_-\mathrm{W}_-) = \frac{g^2}{16\pi}\frac{M_\mathrm{W}^2}{M_\mathrm{H}}\left(1 - \frac{4M_\mathrm{W}^2}{M_\mathrm{H}^2}\right)^{\frac{1}{2}}$$

$$\Gamma(\mathrm{H}^0 \to \mathrm{W_L}\mathrm{W_L}) = \frac{g^2}{64\pi}\frac{M_\mathrm{H}^3}{M_\mathrm{W}^2}\left(1 - \frac{2M_\mathrm{W}}{M_\mathrm{H}^2}\right)^2\left(1 - \frac{4M_\mathrm{W}^2}{M_\mathrm{H}^2}\right)^{\frac{1}{2}}$$

$$\Gamma(\mathrm{H}^0 \to \mathrm{W_L}\mathrm{W}_\pm) = 0.$$

   Hence, for $M_\mathrm{H} \gg M_\mathrm{W}$, the W bosons from Higgs decay are dominantly longitudinally polarized.

2. Show that the amplitude for $\mathrm{W_L^+W_L^-} \to \mathrm{W_L^+W_L^-}$ in the limit where $s, M_\mathrm{H}^2 \gg M_\mathrm{W}^2, M_\mathrm{Z}^2$ is

$$\mathcal{M}(\mathrm{W_L^+W_L^-} \to \mathrm{W_L^+W_L^-}) = -\sqrt{2}Gm_\mathrm{H}^2\left(\frac{s}{s - M_\mathrm{H}^2} + \frac{t}{t - M_\mathrm{H}^2}\right)$$

   with s and t the Mandelstam variables. If $m_\mathrm{H} \to \infty$, the amplitude grows linearly in s. Calculate now the $l = 0$ partial-wave contribution

$$a_0 = \frac{1}{16\pi s}\int_{-s}^{0} \mathrm{d}t\, \mathcal{M}(\mathrm{W_L^+W_L^-} \to \mathrm{W_L^+W_L^-})$$

   and show that, for $s \gg M_\mathrm{H}^2$, the result for a_0 is

$$a_0 = -\frac{GM_\mathrm{H}^2}{8\pi\sqrt{2}}.$$

   This result together with the unitarity condition (17.12) gives Eq. (17.13).

3. A simple estimate of the process of gluon–gluon fusion is obtained by calculating the Drell–Yan process. Consider the reaction $\mathrm{gg} \to \mathrm{H} \to \gamma\gamma$ with the mass M_H varying, i.e. the Higgs is off the mass shell. The point cross section is given in Eq. (17.19) and the decay width is listed in Table 17.1.
   (i) Identify Q^2 in Section 10.5 with M_H^2 and write the Drell–Yan cross section. For the gluon distribution function adopt the simplified form

$$f_\mathrm{g}(x) = 8\frac{1}{x}(1 - x)^7\,.$$

   Compute the production cross section in proton–proton collisions.
   (ii) Compute the cross section numerically for a Higgs of 130 GeV for pp collisions of center-of-mass energy 5–20 TeV. To simplify the calculation, you may treat $I(\lambda)$ with $\lambda = m_\mathrm{t}^2/m_\mathrm{H}^2$ as constant.

https://doi.org/10.1017/9781009402378.018 Published online by Cambridge University Press

References

Bardeen, W. A., Hill, C. T., and Lindner, M. (1996), *Phys. Rev.* **D41**, 1647
Bardin, D., and Passarino, G. (1999), *The Standard Model in the Making* (Oxford, Oxford Science Publications)
Cahn, R. N., and Dawson, S. (1984), *Phys. Lett.* **B136**, 196
Erler, J., and Langacker, P. (2004), *Phys. Lett.* **B592**, 144
Fahri, E., and Susskind, L. (1979), *Phys. Rev*. **D20**, 3404
Gluck, M., Jimenez-Delgado, P., and Reya, E. (2005), *Phys. Rev. Lett.* **95**, 022002, and references therein
Gunion, J. F., Haber, H. E., Kane, G., and Dawson, S. (1990), *The Higgs Hunter's Guide* (New York, Addison-Wesley); Section 2.1 (for decays) and p. 139 (for Higgs production)
Hinchlife, I. (1998), *Eur. Phys. J.* **C3**, 1
Kniehl, B. (1994), *Phys. Rep*. **240**, 211
Lee, B. W., Quigg, C., and Thacker, G. B. (1977a), *Phys. Rev. Lett.* **38**, 833
(1977b), *Phys. Rev.* **D16**, 1519
Linde, A. D. (1976), *JETP Lett.* **23**, 64
Jones, D. R. T., and Petkov, S. T. (1979), *Phys. Lett.* **B84**, 440
Wilczek, F. (1977), *Phys. Rev. Lett.* **39**, 1304

Select bibliography

Roth, S. (2007), *Precision Electroweak Physics at Electron–Positron Colliders* (Berlin, Springer-Verlag)